Polymer–Protein Interaction, Water Retention, and Biocompatibility of a Stimuli-Sensitive Superporous Hydrogel Containing Interpenetrating Polymer Networks

Lichen Yin,[1] Ziming Zhao,[2] Yizhe Hu,[3] Jieying Ding,[2] Fuying Cui,[2] Cui Tang,[1] Chunhua Yin[1]

[1]*State Key Laboratory of Genetic Engineering, School of Life Sciences, Fudan University, Shanghai 200433, China*
[2]*Department of Biochemistry, School of Life Sciences, Fudan University, Shanghai 200433, China*
[3]*Department of Material Science, Fudan University, Shanghai 200433, China*

Received 25 May 2007; accepted 10 November 2007
DOI 10.1002/app.27744
Published online 23 January 2008 in Wiley InterScience (www.interscience.wiley.com).

ABSTRACT: The swelling of a superporous hydrogel containing poly(acrylic acid-*co*-acrylamide)/*O*-carboxymethyl chitosan interpenetrating polymer networks (SPH-IPN) was sensitive toward the pH, ionic strength, and temperature stimuli. With insulin as a model drug, polymer–protein interaction was detected, and it was physical rather than covalent. Freezing water was the majority of the imbibed water in the swollen SPH-IPNs, and the water-retention ability of the polymer against compression and time of exposure at 37°C was improved as the amount of the *O*-carboxymethyl chitosan network increased. A 3-(4,5-dimethylthiazol-2-yl)-2,5-diphenyl tetrazolium bromide (MTT) assay on AD293 and RBL-2H3 cells and an *in situ* lactate dehydrogenase assay and morphological study on rat intestine confirmed that the SPH-IPNs had satisfactory biocompatibility. These pronounced properties suggested that the SPH-IPNs could be developed as an attractive peroral delivery vehicle for peptide and protein drugs. © 2008 Wiley Periodicals, Inc. J Appl Polym Sci 108: 1238–1248, 2008

Key words: biocompatibility; interpenetrating networks (IPN); stimuli-sensitive polymers

INTRODUCTION

Superabsorbent hydrogels have been widely applied recently as soil conditioners, disposable diapers, and absorbent pads.[1–3] Apart from their abilities to absorb and hold large amounts of water, they also present desired characteristics such as fast water absorption, highly porous structures, and excellent mechanical properties for further applications in biomedical and pharmaceutical fields. Among them, porous scaffolds for cell growth[4,5] and superporous hydrogels for peptide drug delivery[6,7] display distinct advantages, in that porous scaffolds provide adequate sites for cell attachment and growth, whereas superporous hydrogels help open the intestinal epithelial tight junctions and facilitate drug absorption through mechanical fixation.

In our previous investigation,[8] a superporous hydrogel containing poly(acrylic acid-*co*-acrylamide)/*O*-carboxymethyl chitosan interpenetrating polymer networks (SPH-IPN) was synthesized. With the introduction of the full interpenetrating network (IPN) structure, high mechanical strength was achieved without the loss of high porosity and fast swelling. SPH-IPNs were ionized hydrogels whose swelling behaviors depended on the characteristics of the external solutions, such as the pH, temperature, and ionic strength. Moreover, SPH-IPNs had higher porosity and larger pore sizes, which might affect the protein loading into and release from the hydrogel. The polymer–protein interactions influenced the protein loading capacity, release kinetics, and protein release mechanisms.[9]

Investigation of the physical state of water in swollen SPH-IPNs was deemed meaningful because it played an important role in enzymatic catalysis, protein and enzyme activity,[10] and drug delivery behavior.[11] Water in the polymer was usually categorized into three types: free water, which froze at the usual freezing point; freezing bound water, which froze at a temperature lower than the usual freezing point, and nonfreezing bound water, which could not freeze at the usual freezing point.[12] The sum of free water and freezing bound water was regarded as freezing water. Various techniques[13–15] had been successfully employed to study the water state, among which differential scanning calorimetry (DSC) could differentiate and determine the relative contents of freezing and nonfreezing bound water in the polymer.[9] Besides, because of the full IPN

Correspondence to: C. Tang (tangcui@fudan.edu.cn) or C. Yin (chyin@fudan.edu.cn).

Contract grant sponsor: Science and Technology Commission of Shanghai Municipality of China; contract grant number: 054319934.

structure, the SPH-IPNs exhibited high mechanical and elastic properties, which were expected to enhance their water-retention capacities.

The majority of publications about superporous hydrogels emphasize their high swelling capacities and mechanical properties without a focus on essential features such as stimuli-sensitive swelling, polymer–protein interactions, water state, water-retention capacities, and biocompatibility, which were highly demanded when the polymers were developed as a potential peroral delivery system for protein drugs. Therefore, the pH, salt, and thermosensitive swelling of the SPH-IPNs were investigated in this study. Polymer–protein interactions were studied via insulin loading and release with respect to different insulin concentrations of the loading solutions. Water retention of the polymer with response to compression and time of exposure at 37°C was evaluated, and the water state in both blank and insulin-loaded SPH-IPNs was analyzed with DSC. Biocompatibility of the SPH-IPNs was further evaluated with a 3-(4,5-dimethylthiazol-2-yl)-2,5-diphenyl tetrazolium bromide (MTT) assay on AD293 and RBL-2H3 cells and with an *in situ* lactate dehydrogenase (LDH) assay and histological damage on rat intestine.

EXPERIMENTAL

Materials

SPH-IPNs were synthesized in our laboratory as described previously,[8] and samples with *O*-carboxymethyl chitosan (*O*-CMC)/monomer ratios (w/w) of 0.048, 0.096, 0.144, and 0.192 were designated SPH-IPN_{48}, SPH-IPN_{96}, SPH-IPN_{144}, and SPH-IPN_{192}, respectively. Monocomponent insulin crystals (28 IU/mg) were purchased from Xuzhou Biochemical Co. (Xuzhou, China). Carbomer was donated by BF Goodrich (Cleveland, OH). MTT was purchased from Sigma (St. Louis, MO). The human embryonic kidney cell line AD293 and the rat basophilic leukemia cell line RBL-2H3 were obtained from the American Type Culture Collection (Rockville, MD) and were cultured in Dulbecco's modified Eagle medium (DMEM; Gibco, Grand Island, NY) containing 10% (v/v) heat-denatured fetal calf serum, 1% (v/v) nonessential amino acids, 160 U/mL benzylpenicillin, and 100 U/mL streptomycin (Sigma, St. Louis, MO). Acetonitrile (Merck, Darmstadt, Germany) was high-performance liquid chromatography (HPLC) grade. Other chemicals were analytical-grade.

Stimuli-sensitive swelling measurements

To determine the effects of the ionic strength, pH, and temperature on the hydrogel swelling kinetics, NaCl solutions with ionic strengths of 0.0001–1*M* (pH 7.0), HCl or NaOH solutions with defined pHs from 1.0 to 7.4, and deionized water at 20, 30, and 40°C were used as the swelling media, respectively. Forty milligrams of dried SPH-IPN_{144} was allowed to hydrate in 300 mL of the swelling medium. At time intervals, the weight of the swollen hydrogel was measured after the excessive surface swelling medium was blotted. The swelling ratio (Q_s) was defined as follows:

$$Q_s = (W_s - W_d)/W_d \quad (1)$$

where W_d denotes the weight of the dried hydrogel and W_s is the weight of the swollen hydrogel at certain time intervals.

Pulsatile pH-dependent swelling of the SPH-IPNs was evaluated at 37°C with alternation of the swelling medium between the HCl solution (pH 1.0) and phosphate buffered solution (PBS; pH 7.4). The SPH-IPNs were brought into swelling equilibrium in PBS before being transferred to the HCl solution. The swollen hydrogels in the HCl solution were weighed at each given time and transferred to the PBS buffer when no further changes in the swelling ratios over time were confirmed. The same procedures were performed for swelling in PBS before the swollen hydrogels were transferred back to the HCl solution.

Fourier transform infrared (FTIR) spectroscopy

Samples swollen in HCl (pH 1.0) and PBS (pH 7.4) were vacuum-dried and powdered, respectively. The FTIR spectrum was recorded over the range of 400–4000 cm^{-1} in a Nexus 470 FTIR spectrometer (Nicolet, Madison, WI).

Scanning electron microscopy (SEM)

To examine the morphological integrity of the polymer after reversible swelling, SPH-IPNs taken from the HCl solution or PBS were rapidly frozen in liquid nitrogen and thereafter lyophilized to prevent the collapse of the porous structure. The inner surface of the lyophilized polymer was exposed and imaged in an S-520 scanning electron microscope (Hitachi, Tokyo, Japan).

Polymer–protein interactions

Insulin loading

Thirty milligram of the SPH-IPN was placed in a 4-mL insulin solution (dissolved in 0.01*M* PBS) for 4 h at 37°C. The total amount of insulin loaded was determined by the mass change of insulin in the solution before and after loading. The insulin content in the loading solution was analyzed by HPLC as described previously.[8] The experimental and theoretical

loadings were calculated with the following equations:

$$\text{Experimental loading (\%)} = (M_{\text{total}} - M_{\text{residual}}) \times 100/M_{\text{total}} \quad (2)$$

$$\text{Theoretical loading (\%)} = vC \times 100/M_{\text{total}} \quad (3)$$

where M_{total} and M_{residual} stand for the masses of insulin in the solution before and after loading, respectively (mg); v represents the volume of the insulin solution absorbed by the hydrogel (mL); and C is the concentration of the insulin solution used for loading (mg/mL).

In vitro release

The insulin-loaded SPH-IPNs were vacuum-dried until they reached a constant weight. The dried hydrogels, loaded with different amounts of insulin, were immersed in 25 mL of 0.01*M* PBS (pH 7.4), and *in vitro* release was carried out in a glass bottle that was kept at 37°C and shaken at 150 rpm. At time intervals, 150-μL aliquots of the release medium were taken out, after which 150 μL of PBS was added to maintain a constant volume. To quantitatively analyze the residual amount of insulin, the SPH-IPNs after *in vitro* release were vacuum-dried and crushed into fine powders before being reconstituted in PBS. The insulin concentration was analyzed by HPLC as mentioned previously.

Structural integrity of insulin in SPH-IPNs

Insulin-loaded SPH-IPN$_{144}$ after *in vitro* release was subjected to excessive washing with PBS to remove noncovalent adsorption of insulin to polymeric matrices. FTIR spectra of solid insulin, SPH-IPN$_{144}$, insulin-loaded SPH-IPN$_{144}$, and washed SPH-IPN$_{144}$ were then recorded over the range of 400–4000 cm^{-1} in a Nexus 470 FTIR spectrometer (Nicolet).

State of water in SPH-IPNs

SPH-IPNs were swollen to equilibrium in water at 37°C. The equilibrium water content (EWC) was calculated as follows:

$$\text{EWC (\%)} = (W_e - W_d) \times 100/W_e \quad (4)$$

where W_e is the weight of the swollen state at equilibrium and W_d is the weight of the dry hydrogel.

Ten milligrams of the fully swollen SPH-IPN was sealed in a differential scanning calorimeter (2910M, TA Instruments, New Castle, DE) aluminum sample pan, which was cooled to −40°C and then heated to 30°C at a heating rate of 5°C/min under a 60 cc/min nitrogen gas flow. The amount of bound water in the SPH-IPN could be calculated from the following equation under the condition that the heat of fusion of free water in the hydrogel was the same as that of the ice:[16,17]

$$W_b\ (\%) = \text{EWC}\ (\%) - (W_f + W_{fb})\ (\%) = \text{EWC}\ (\%) - (Q_{\text{endo}}/Q_f \times 100)\ (\%) \quad (5)$$

where W_b, W_f, and W_{fb} represent the amounts of nonfreezing bound water, free water, and freezing bound water, respectively. Q_{endo} (J/g) is the heat of fusion of free water in the hydrogel (obtained from the area of the endothermic peak around 0 and 10°C). Q_f (J/g) is the heat of fusion of pure water.[9]

Water retention

The water-retention capacity with respect to compression (WR_c) of the SPH-IPNs was evaluated with a comparator bench at the ambient temperature. The fully swollen SPH-IPN, supported by a Petri dish, was put longitudinally under the lower touch. Weights were applied to the upper touch, whereas the weight of the hydrogel under each determined compressive pressure was measured.

For the investigation of the water-retention capacity as a function of the time of exposure at 37°C (WR_t) of the SPH-IPNs, the water loss of the fully swollen polymer at timed intervals was determined by gravimetry.

The following equation was used to determine the water-retention capacity (WR) of the SPH-IPNs:

$$\text{WR} = (W_p - W_d)/(W_s - W_d) \quad (6)$$

where W_d is the weight of the dried hydrogel, W_s is the weight of the fully swollen hydrogel, and W_p is the weight of the hydrogel under different compressive pressures or at various exposure times.

Biocompatibility

Cytotoxicity

AD293 cells and RBL-2H3 cells were seeded onto 96-well culture plates at a density of 1×10^4 cells per 200 μL per well in DMEM and subsequently cultured in a humidified atmosphere of 5% CO_2 at 37°C for 24 h. For direct cell–material contact, 2 mg of SPH-IPN$_{192}$ was fully swollen in DMEM and then added to the wells. For indirect cell–material contact, 40 mg of SPH-IPN$_{192}$ was allowed to swell in 4 mL of DMEM for 3 days. The obtained gel extract was filter-sterilized (0.22-μm pore size), and 100 μL of it was added per well. For a negative control, no polymer was added, whereas for an internal reference,

100 μL of 0.5% (w/v) carbomer in DMEM was applied to the cells. Cells were further incubated for 4 h, and the cell viability was quantitatively analyzed by the MTT assay.

Biochemical evaluation of intestinal damage

Animal experiments complied with the guiding principles for the care and use of laboratory animals at Fudan University. Male Sprague–Dawley rats weighing 200–250 g were anesthetized by an intraperitoneal injection of 40 mg of sodium pentobarbital/kg of body weight and placed on a heating pad to maintain a body temperature of 37 ± 1°C. Following a midline incision in the abdomen, a 5-cm jejunum loop was identified and washed gently with prewarmed PBS to remove intestinal content. Five micrograms of SPH-IPN$_{192}$ was administered to the jejunum loop with 1 mL of PBS. One milliliter of PBS served as a negative control, whereas 1 mL of 1% (w/v) sodium glycocholate served as a positive control. After incubation for 2 h in the abdominal cavity, the loop was washed with 1 mL of PBS, and the intestinal fluid was collected to determine the concentration of LDH with an LDH-UV kit (Kangte Biotech Corp., Zhejiang, China).

Histological damage

Three rats orally administered enteric capsules containing 5 mg of SPH-IPN$_{192}$ were sacrificed 2 h after dosing as a test group, and the jejunum in which the polymer was located was excised. Three rats receiving blank capsules were sacrificed 2 h after dosing as a control group, whereas another three rats receiving capsules loaded with SPH-IPN$_{192}$ were sacrificed 48 h after dosing as a refresh group. The separated jejunum was washed with PBS, fixed in a 10% neutral formaldehyde solution, dehydrated in alcohol, fixated in paraffin, and stained with hematoxylin/eosin. Cross sections of the jejunum were examined with a 55i light microscope (Nikon, Tokyo, Japan).

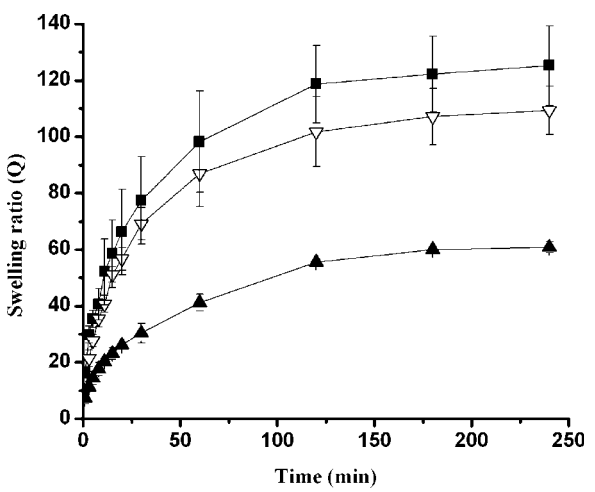

Figure 1 Swelling kinetics of SPH-IPN$_{144}$ in double distilled water (pH 7.4, ionic strength < 0.001*M*) at (▲) 20, (▽) 30, and (■) 40°C (n = 3, mean ± standard deviation).

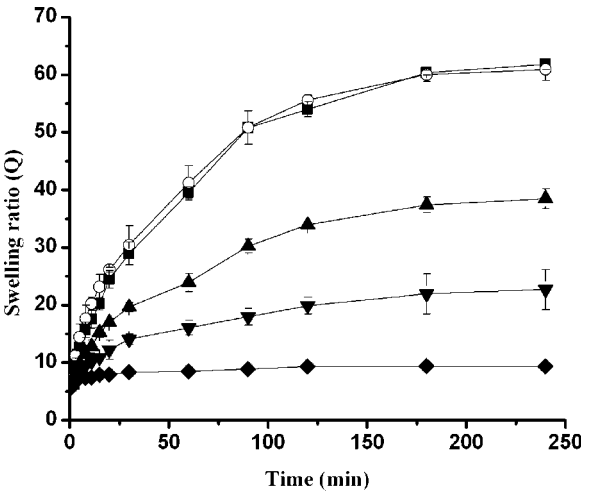

Figure 2 Swelling kinetics of SPH-IPN$_{144}$ at 20°C in NaCl solutions (pH 7.0) with ionic strengths of (◆) 1, (▼) 0.1, (▲) 0.01, (○) 0.001, and (■) 0.0001*M* (n = 3, mean ± standard deviation).

RESULTS AND DISCUSSION

Stimuli-sensitive swelling behaviors

Temperature-sensitive

Swelling behaviors of the SPH-IPNs at different temperatures are shown in Figure 1. As the temperature increased from 20 to 40°C, the polymer swelled faster, and the equilibrium swelling ratio was enhanced accordingly. This was due to the disentanglement of interpenetrated polymeric chains, destruction of hydrogen bonding between polymer molecules, and increased chain mobility at a higher temperature, which facilitated network expansion.[18] Such temperature responsiveness was also attributed to the high porosity of the SPH-IPNs because more pores would enhance the uptake of water during swelling in comparison with less porous hydrogels.[19]

Salt-sensitive

Figure 2 shows that an increase in the ionic strength within the range of 0.001–1*M* yields a significant decrease in the swelling ratio of SPH-IPN$_{144}$. When the ionic strength was no higher than 0.001*M*, it brought about an insignificant difference in the swel-

ling behaviors of the polymer. The sensitive swelling of the anionic SPH-IPNs toward ionic strength was attributed to the change in the charge distribution on the surface of the gel network. As the concentration of cations in the swelling medium increased, a stronger ''charge screening effect''[20] of the additional cations was achieved, causing imperfect anion–anion electrostatic repulsion and a decreased osmotic pressure difference between the polymer network and the external solution. Therefore, swelling of SPH-IPN_{144} was decreased. When the ionic strength was no higher than 0.001*M*, the solution lacked enough ions to shield the polymer chains from one another, leading to an inappreciable influence on the swelling of the SPH-IPNs.

pH-sensitive

The effect of pH on the swelling properties of SPH-IPN_{144} is shown in Figure 3. A drastic increase in the swelling was observed within the pH range of 3.0–6.2, whereas at pH > 6.2 or pH < 3.0, the change in the swelling behavior was slight. At a very acidic condition (pH $\leq$ 3.0), the carboxylic groups on poly (acrylic acid) and *O*-CMC were converted to the protonated acid form, and hydrogen bonds between them were formed; this resulted in the decreased swelling ratio of the hydrogel. A screening effect of the counterions, that is, Cl^-, shielded the charge of the cations ($—NH_2^+$ and $—NH_3^+$) and prevented efficient repulsion.[21] In addition, the high ionic strength of the swelling medium at pHs 1.0 and 3.0 was also responsible for the restricted swelling of the polymer. When the pH exceeded 3.0, the carboxylic acid was gradually ionized to the salt (basic) form.[22]

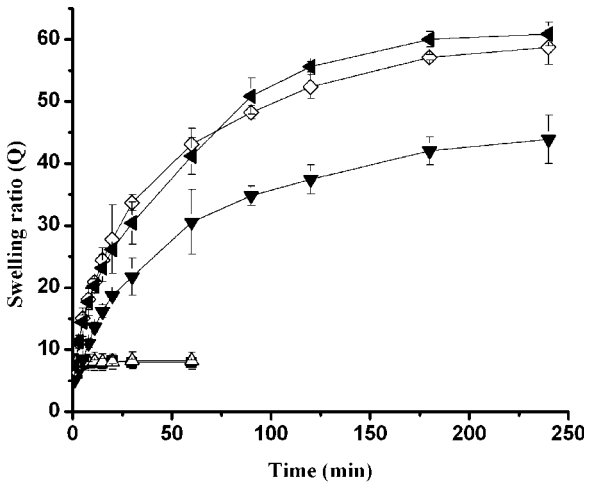

Figure 3 Swelling kinetics of SPH-IPN_{144} at 20°C in HCl or NaOH solutions with pHs of (■) 1.0 (ionic strength = 0.1*M*), (△) 3.0 (ionic strength = 0.001*M*), and (▼) 4.9, (◇) 6.2, and (◀) 7.4 (ionic strength < 0.0001*M* when pH ≥ 4.9; n = 3, mean ± standard deviation).

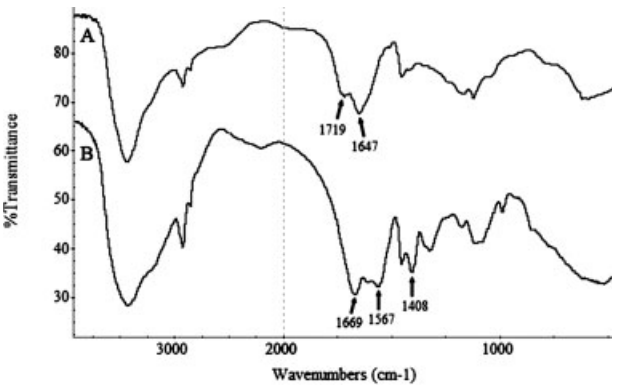

Figure 4 FTIR spectra of SPH-IPN_{144} after swelling in (A) a pH 1.0 HCl solution and (B) pH 7.4 PBS. Swollen samples were vacuum-dried and powdered before FTIR analysis.

With the increase in the electrostatic repulsive force among the COO^- groups and the osmotic pressure inside the hydrogel, swelling of the polymer significantly increased. When the pH reached 6.0, all the carboxylic groups were converted to the salt form, and maximum swelling was obtained; this accounted for similar swelling behaviors at pHs 6.2 and 7.4. The lower ionic strengths of the solutions at pHs 4.9, 6.2, and 7.4 also favored swelling of the SPH-IPN, as mentioned previously.

Figure 4(A,B) depicts the FTIR spectra of SPH-IPN_{144} after it is swollen in an HCl solution (pH 1.0) and PBS (pH 7.4), respectively. Peaks at 1647 [Fig. 4(A)] and 1669 cm^{-1} [Fig. 4(B)] represent the stretching vibration of the carbonyl. The peak at 1719 cm^{-1} [Fig. 4(A)] represents the stretching vibration of the —COOH group and disappears in Figure 4(B). Also, peaks at 1567 and 1408 cm^{-1} [Fig. 4(B)], which refer to asymmetric and symmetric stretching of $—COO^-$ in the associated carboxylic acid salt, respectively, cannot be observed in Figure 4(A). This result indicates that all the carboxyl groups on SPH-IPN are protonated at pH 1.0 but ionized at pH 7.4, and this confirms the previous explanation for the pH-sensitive swelling of the polymer.

Figure 5 shows the swelling reversibility of SPH-IPNs between pH 1.2 and pH 7.4 solutions. Both SPH-IPN_{48} and SPH-IPN_{192} were able to quickly absorb and deabsorb the swelling medium upon the pH change from acidic conditions to basic conditions and vice versa. The structure of the SPH-IPNs with large numbers of pores connected to one another to form capillary channels was favorable for easy diffusion of the swelling medium into the polymeric matrix, thus contributing to its quick response toward pH change. The time for swelling was longer than that for deswelling of the hydrogels, and the swelling rate of SPH-IPN_{192} in a basic external solution

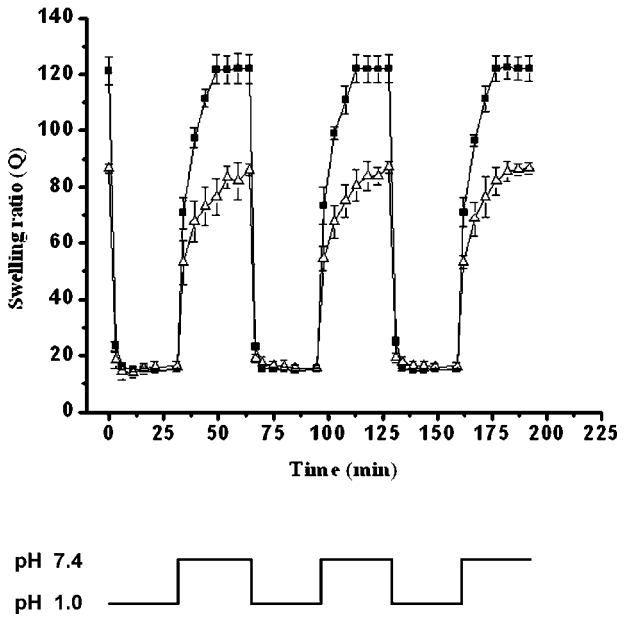

Figure 5 Pulsatile pH-dependent swelling behaviors of (■) SPH-IPN$_{48}$ and (△) SPH-IPN$_{192}$ at 37°C with alternation of the swelling medium between an HCl solution (pH 1.0) and PBS (pH 7.4; n = 3, mean ± standard deviation).

was slower than that of SPH-IPN$_{48}$. This might be due to the restricted chain mobility of poly(acrylic acid-*co*-acrylamide) [P(AA-*co*-AM)], which was anchored at several points through molecular entanglement with the crosslinked *O*-CMC network, because the fast pH-sensitive behavior of hydrogels was based on the freely mobile side chains.[8,23]

As shown in Figure 6, the porous structure of the SPH-IPNs remained intact and undestroyed after several swelling–deswelling cycles. Such a result would account for the fact that the pulsatile swelling process could be repeated even more times with excellent reproducibility and fast response (data not shown).

Polymer–protein interactions

Insulin loading

The ability to load different doses of proteins was deemed an important aspect when hydrogels were used as protein delivery devices. Protein loading into and release from a hydrogel was controlled by the pore volume fraction, the pore sizes and their interconnections, and the interactions between the protein and polymer chains.[9] When the insulin concentration of the loading solution varied from 0.1 to 1.5 mg/mL, greater discrepancies between the theoretical and experimental loading levels were observed for both SPH-IPN$_{48}$ and SPH-IPN$_{192}$ (Table I). These disparities may be attributed to the strong affinity between the insulin and the gel matrix. Large numbers of interconnected pores led to the large inner surface area, facilitating easy adsorption

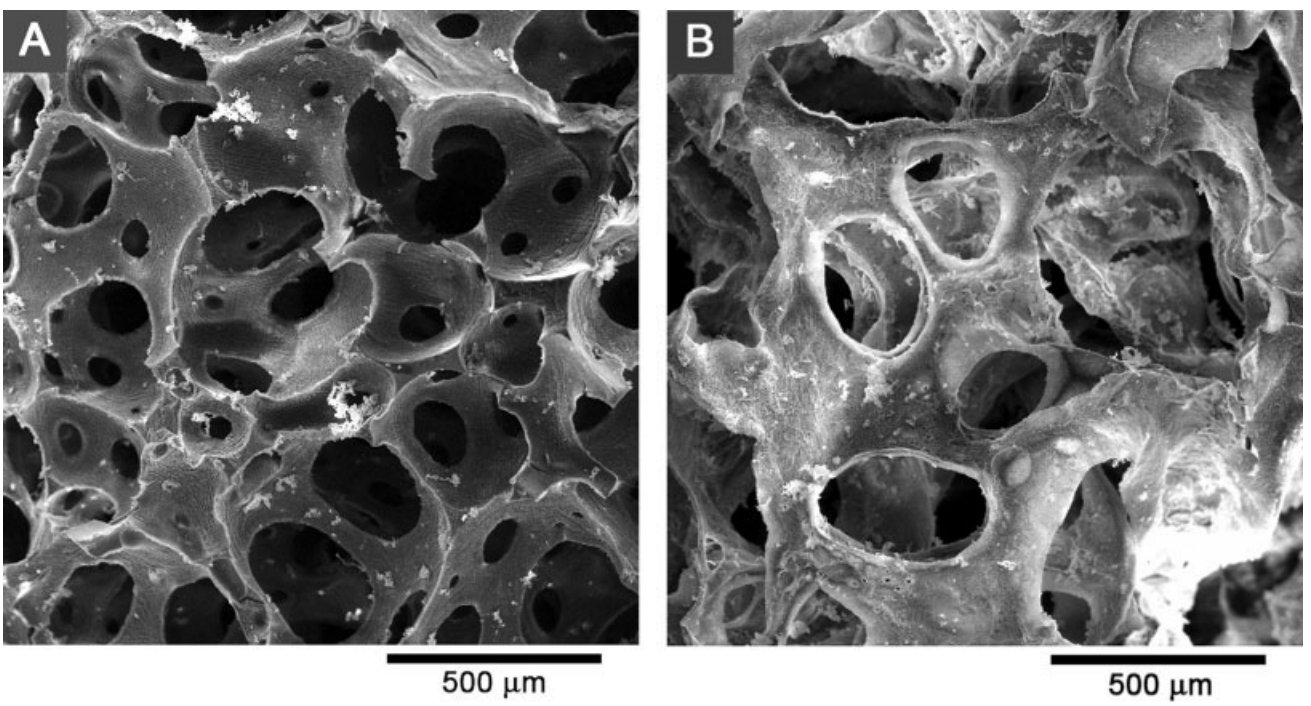

Figure 6 SEM images of SPH-IPNs after pulsatile swelling in (A) an HCl solution (pH 1.0) and (B) PBS (pH 7.4). Samples were taken from the respective solutions after several cycles of pulsatile swelling and were lyophilized before morphological examination.

TABLE I
Insulin Loading into SPH-IPNs

Gel sample	Insulin concentration (mg/mL)	Drug loading (%)		
		Theoretical	Experimental	Difference[a]
$SPH\text{-}IPN_{48}$	0.1	34.8	89.0	54.2
	0.5	34.0	93.1	59.1
	1.5	31.7	96.7	65.0
$SPH\text{-}IPN_{192}$	0.1	32.3	81.2	48.9
	0.5	31.9	81.1	49.2
	1.5	29.8	92.4	62.6

[a] Difference in the percentage protein loadings of the theoretical and experimental levels.

of insulin onto it. Electrostatic interaction and hydrogen bonding between insulin and the ionized groups on the polymeric chains also contributed to the higher amount of protein actually loaded into the gel matrix versus the theoretical amount. Less insulin was loaded into $SPH\text{-}IPN_{192}$ than into $SPH\text{-}IPN_{48}$ because of the reduced swelling ratio as the amount of *O*-CMC increased.[8]

In vitro release

As shown in Figure 7, more than 90% of the insulin loaded could be released within 2 h, and a faster release rate was achieved as the initial loading level was enhanced. The fast swelling and large swelling ratio of the polymer accounted for the fast release of proteins. The significantly smaller molecular size of insulin in its globular form versus the pore size of swollen SPH-IPNs, which was several hundred micrometers, enabled it to diffuse through the gel network with greater ease. The increased amount of encapsulated proteins also created an enhanced diffusion driving force of the concentration gradient, thus leading to faster protein release. Insulin could be quickly released from the SPH-IPNs, and the amount of residual protein was low; this indicated that the interaction between insulin and the SPH-IPNs was physical rather than covalent.

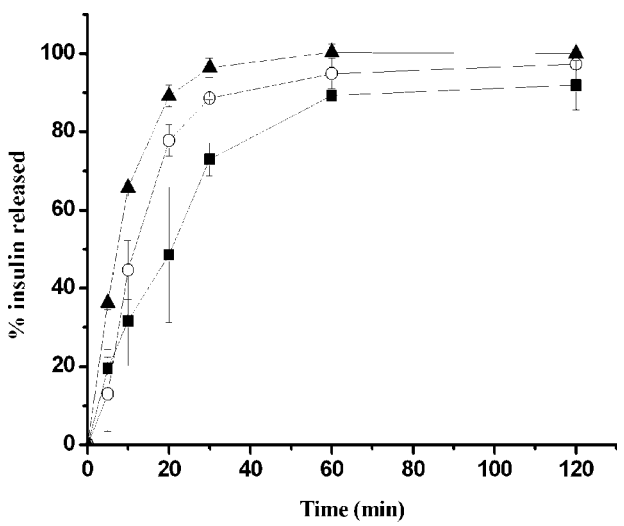

Figure 7 Effect of the insulin concentration in the loading solution on protein release from $SPH\text{-}IPN_{144}$ in PBS at 37°C: (■) 0.1, (○) 0.5, and (▲) 1.5 mg/mL.

Insulin integrity in SPH-IPN

In the FTIR spectrum of insulin [Fig. 8(A)], four peaks were observed at 3336, 1649, 1518, and 1240 cm^{-1}, which referred to amides A, I, II, and III, respectively. $SPH\text{-}IPN_{144}$ showed five peaks at 3437, 1648, 1451, 1166, and 1039 cm^{-1} [Fig. 8(B)], which were related to the —O—H stretching, antisymmetric stretching and symmetric stretching of $—COO^-$ in the associated carboxylic acid salt, C—O stretching of the secondary hydroxyl group (—CH—OH) in cyclic alcohols, and C—O stretching of the primary hydroxyl group ($—CH_2—OH$) in primary alcohols, respectively. After loading with insulin, the peaks at 1166 and 1039 cm^{-1} in the spectrum of $SPH\text{-}IPN_{144}$ were replaced by a strong band at 1072 cm^{-1} [Fig. 8(C)], and no other new peaks were detected. However, the spectrum of washed $SPH\text{-}IPN_{144}$ [Fig. 8(D)] appeared similar to that of $SPH\text{-}IPN_{144}$. Such a difference indicated that the peak at 1072 cm^{-1} might be due to physical rather than covalent interactions between insulin and the polymer, such as hydrogen bonds or electrostatic interaction, and this was in accordance with the results in the previous literature[24] and in the *In Vitro* Release section. The absence of covalent polymer–protein interactions also accounted for the complete and rapid release of insulin in PBS.

State of water

According to the three-state water model in gels,[16] water molecules first disrupt the intermolecular hydrogen bonds and then bind to the hydrophilic

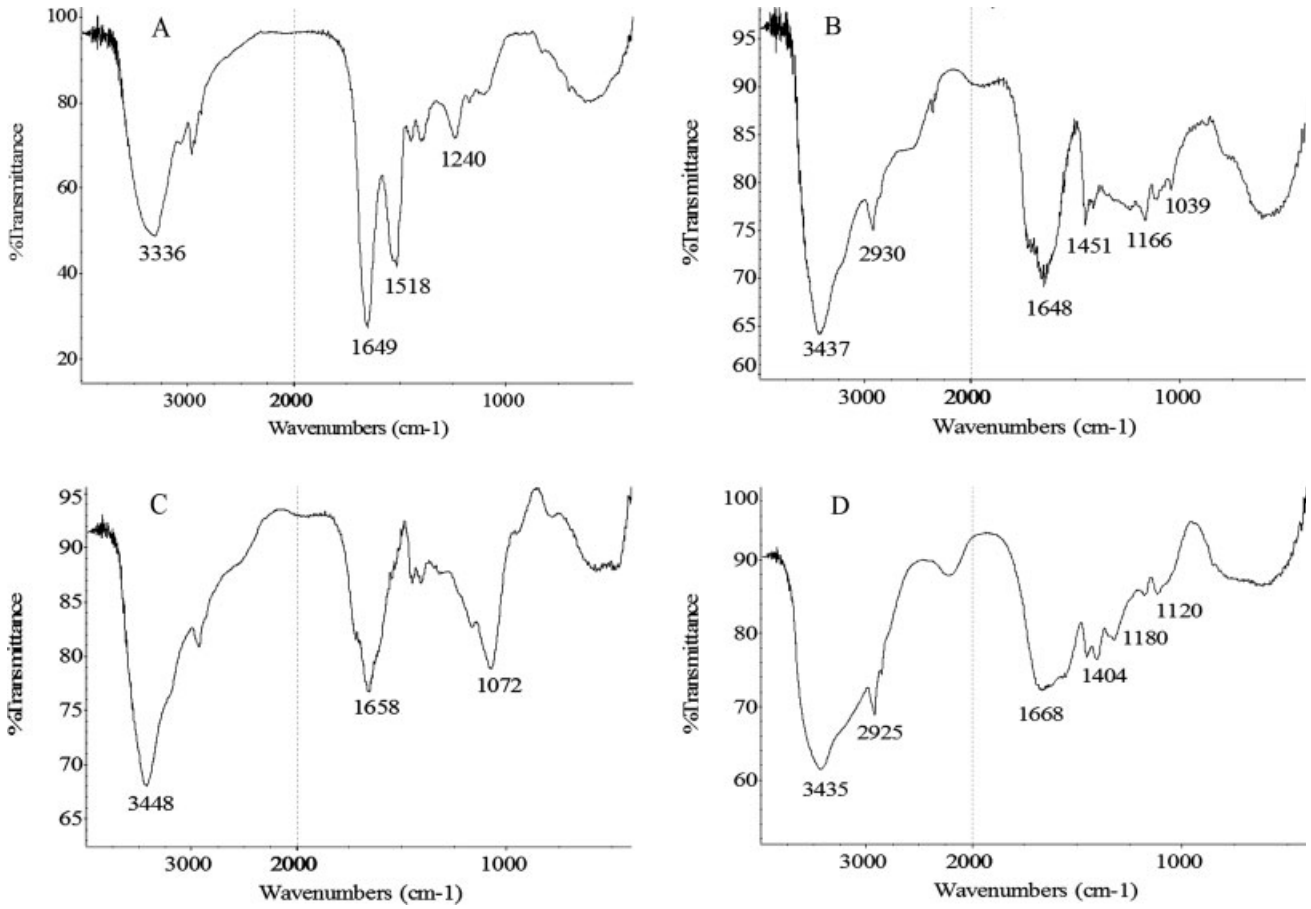

Figure 8 FTIR spectra with respect to the integrity of insulin in the SPH-IPN polymeric matrix: (A) insulin, (B) SPH-IPN$_{144}$, (C) insulin-loaded SPH-IPN$_{144}$, and (D) washed SPH-IPN$_{144}$.

sites in the initial swelling process. These water molecules, which are isolated and uniformly distributed throughout the polymer, have greatly restricted mobility and are called nonfreezing bound water. They usually have strong interactions with the polar and hydrophilic groups of the polymer in the form of ion–dipole, dipole–dipole, and hydrogel bonding.[25] Above a certain level of bound water, the additional water is preferentially oriented around the bound water and the polymer network structure as a secondary or tertiary hydration shell, which is in a form generally called clusters. These cagelike structures result from the tendency of water molecules to form the maximum number of hydrogen bonds in the available space. This type of water is called freezing bound water. As the hydrogel gradually approaches the equilibrium water uptake, the freezing water (freezing bound and free water) portion becomes more and more predominant,[16] of which free water is the majority that is not involved in the formation of hydrogen bonding with polymer molecules.

As shown in Table II, freezing water was the major component of the imbibed water in both swollen SPH-IPN$_{48}$ and SPH-IPN$_{192}$. The mass ratio of the bound water to the polymer, which authentically represented the ability of the polymer to form hydrogen bonding with water molecules, decreased as the content of *O*-CMC increased. The greater hydration ability and easier accessibility for hydration of hydrophilic SPH-IPN resulted in the higher freezing water content in the swollen SPH-IPN.[17]

TABLE II
Contents of Freezing and Bound Water in Blank and Insulin-Loaded SPH-IPNs

Gel sample[a]	EWC (%)	W_b (%)	W_f (%)	Bound water/polymer (w/w)
SPH-IPN$_{48}$/0	99.2	15.1	84.1	18.9
SPH-IPN$_{192}$/0	98.8	20.3	78.5	16.9
SPH-IPN$_{192}$/1.5	97.5	32.9	64.6	13.2
SPH-IPN$_{192}$/3.0	97.5	25.0	72.5	10.0
SPH-IPN$_{192}$/5.0	97.4	21.3	76.1	8.2

[a] SPH-IPN$_{48}$/0 and SPH-IPN$_{192}$/0 refer to blank gel samples, whereas SPH-IPN$_{192}$/1.5, SPH-IPN$_{192}$/3.0, and SPH-IPN$_{192}$/5.0 represent insulin-loaded gel samples in which the insulin concentrations of the loading solutions were 1.5, 3.0, and 5.0 mg/mL, respectively.

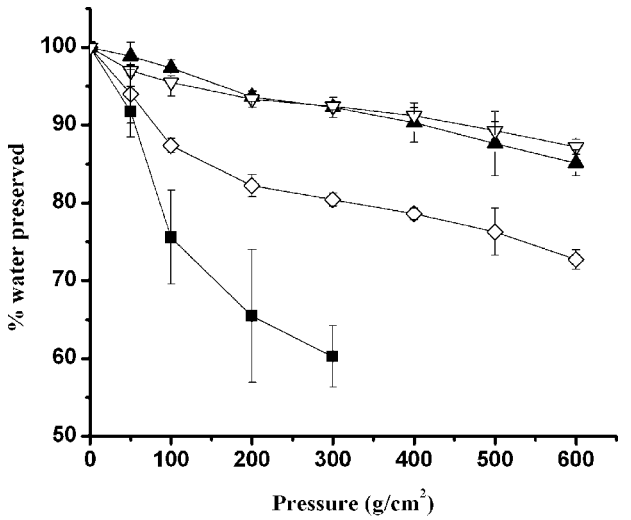

Figure 9 WR_c of SPH-IPNs: (■) SPH-IPN_{48} (the polymer completely fractured when the applied pressure exceeded 300 g/cm^2), (◇) SPH-IPN_{96}, (▲) SPH-IPN_{144}, and (▽) SPH-IPN_{192} (n = 4, mean ± standard deviation). WR_c is expressed as the percentage of water retained in the polymer under a certain compressive force.

The competition of intermolecular hydrogen bonding between P(AA-*co*-AM) and *O*-CMC greatly interfered with the interaction between the polymer and water molecules, which contributed to a decrease in the percentage of bound water. Besides, the crosslinked *O*-CMC provided fewer hydrogen bonding sites and ionic functional residues (—OH and —COOH) than P(AA-*co*-AM), leading to a decreased mass ratio of the bound water to the polymer as the content of *O*-CMC increased.

The insulin-loaded SPH-IPN_{192} possessed a lower mass ratio of the bound water to the polymer than blank SPH-IPN_{192}, and it was further decreased as the insulin concentration of the loading solution increased (Table II). The decreased water binding ability of the insulin-loaded SPH-IPN_{192} was possibly attributable to the significant interactions between the proteins and the gel, which led to the unavailability of existing binding sites for water molecules within the gel network.

Water retention

Figure 9 depicts the water retention of the SPH-IPNs under different compressive pressures. An increase in the *O*-CMC/monomer ratio led to enhanced WR_c of the corresponding polymer, whereas WR_c of SPH-IPN_{144} and SPH-IPN_{192} showed no significant difference ($p > 0.05$). Under a compressive pressure of 600 g/cm^2, WR_c of SPH-IPN_{96}, SPH-IPN_{144}, and SPH-IPN_{192} was 73, 85, and 87%, respectively (SPH-IPN_{48} was completely fractured under 300 g/cm^2). The full IPN structure, within which crosslinked *O*-CMC appeared as a netlike distribution, brought about decreased polymer rigidity, thus improving the resiliency of the polymer in response to compression and efficiently preventing water loss. Furthermore, entanglement of crosslinked *O*-CMC and P(AA-*co*-AM) led to an enhanced amount of net points and mesh units, which favored entrapment of water.[26] The high water affinity of *O*-CMC could also account for the improved water-retention ability.

Figure 10 shows that both SPH-IPN_{48} and SPH-IPN_{192} lost most of the freezing water after exposure to 37°C for 16 h. SPH-IPN_{192} exhibited slower water loss and a higher amount of retained water in comparison with SPH-IPN_{48}, and this suggested that a higher content of the *O*-CMC network was favorable for WR_t of the SPH-IPNs. WR_t of the SPH-IPNs could be attributed to the hydrophilic branch chains of P(AA-*co*-AM) and *O*-CMC, which created a hydrophilic environment, thus minimizing water loss from the hydrogel. The interconnected pores allowed the polymer to hold more water by capillary force.[2] As for SPH-IPN_{192}, the lower proportion of free water that was highly mobile and could be easily lost accounted for its improved WR_t.

Biocompatibility

As illustrated in Figure 11, no adverse effects on the viability of AD293 or RBL-2H3 cells were observed after either direct or indirect contact with SPH-IPN_{192}. No significant difference ($p > 0.05$) was detected in comparison with the negative control. Moreover, the cells attached and spread, with no morphological alteration (data not shown). As

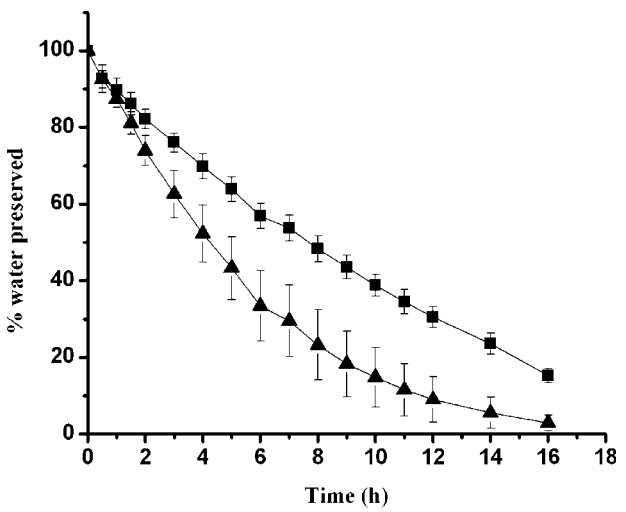

Figure 10 WR_t of SPH-IPNs: (▲) SPH-IPN_{48} and (■) SPH-IPN_{192} (n = 4, mean ± standard deviation). WR_t is expressed as the percentage of water retained in the polymer at certain time intervals.

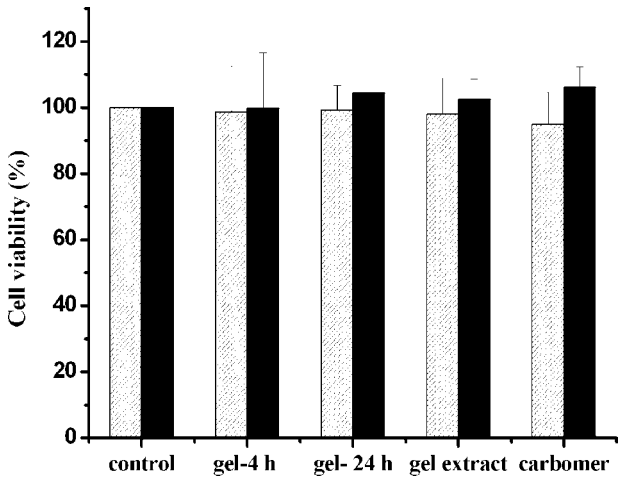

Figure 11 *In vitro* cytotoxicity of SPH-IPN$_{192}$ toward (■) AD293 cells and (□) RBL-2H3 cells by MTT assay. Cells treated with the culture medium were assumed to have 100% cell viability. The gel-4 h and gel-24 h groups had cell–gel direct contact for 4 and 24 h, respectively. Data are expressed as the mean ± standard deviation of four to six experiments.

reported previously,[8] synthesized SPH-IPNs were extensively dialyzed against an HCl solution and ethanol. Residual monomers, initiators, and crosslinkers, which were mainly responsible for the cytotoxicity of the synthesized polymers, could meanwhile be completely removed.

According to the LDH assay, LDH leakage following 2-h administration of PBS, SPH-IPN$_{192}$, and a glycocholate solution was 1.06 ± 0.33, 1.12 ± 0.30, and 3.10 ± 0.60 U (n = 6), respectively. LDH leakage was dramatically induced by the administration of a typical penetration enhancer, 1% sodium glycocholate, in comparison with the negative control ($p < 0.001$), and this demonstrated the occurrence of epithelium membrane damage and cell death. As for SPH-IPN$_{192}$, LDH was negligibly leaked into the jejunum loop, and this was similar to the negative control ($p > 0.05$), suggesting that the polymer induced no mucosal damage and that the intestinal epithelia remained intact.

Figure 12 shows typical cross sections of the rat jejunum. In the control group [Fig. 12(A)], in which no polymer was administered, villi in the intestinal lumen and at the mucosal surfaces were intact. In the test group [Fig. 12(B)], in which SPH-IPN was applied, the villi remained intact, but because of swelling of the polymer and subsequent attachment onto the intestinal epithelium, a few of the cells were detached from the tip of villi. Such detachment was insignificant in comparison with the control [Fig. 12(A)] and could be recovered 48 h later [Fig. 12(C)] because of fast regeneration of the mucous membrane.

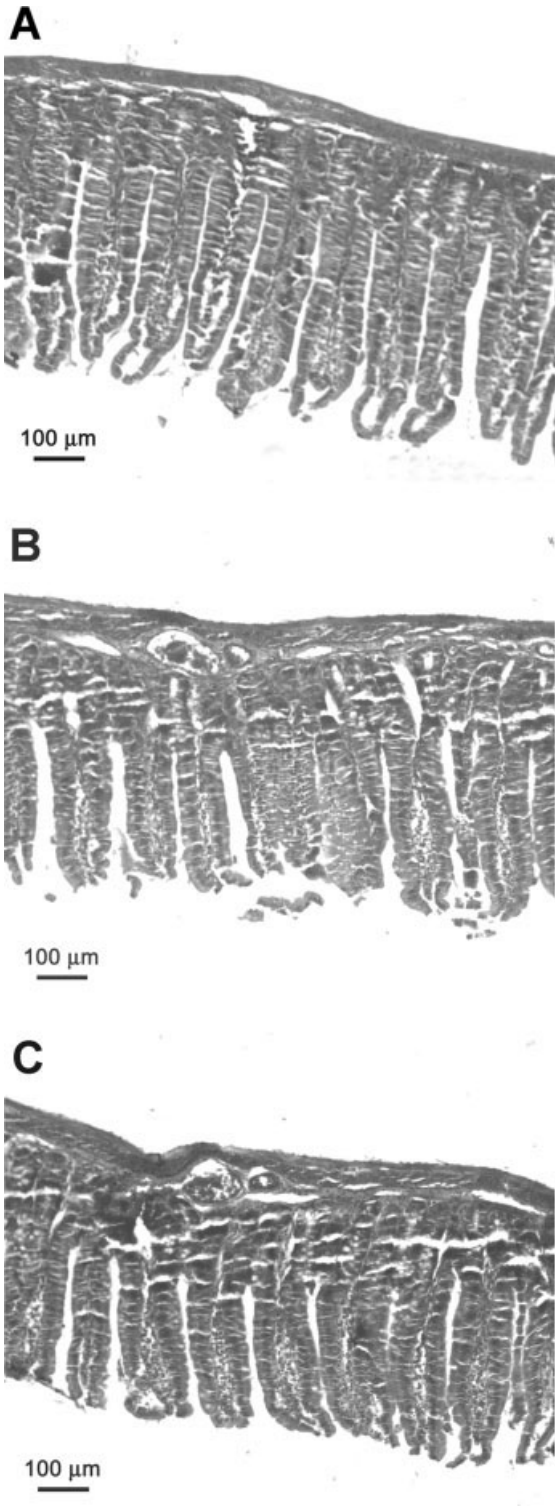

Figure 12 Light microscopy pictures of typical cross sections of rat jejunum (magnification: 100×): (A) rats of the control group administered blank capsules, (B) rats of the test group sacrificed 2 h after capsules loaded with SPH-IPN were administered, and (C) rats of the refresh group sacrificed 48 h after capsules loaded with SPH-IPN were administered.

CONCLUSIONS

Swelling of the SPH-IPNs was significantly affected by the external pH, ionic strength, and temperature stimuli. The equilibrium swelling ratios exhibited high values at low ionic strengths or at pHs 6.2 and 7.4 because of the ionization of the —COOH groups in the SPH-IPNs. The SPH-IPNs exhibited responsiveness toward temperature changes because of the increased chain mobility at a higher temperature. Because of the superporous structure, the SPH-IPNs could also rapidly reach equilibrium swelling and deswelling states with pH changes between acidic and neutral conditions. The significant difference between the experimental and theoretical loading efficiencies for insulin implied the presence of strong polymer–protein interactions, whereas the fast and complete release of insulin from the hydrogels indicated that such interaction was physical rather than covalent, and this was further confirmed by FTIR analysis. Besides, insulin release from the SPH-IPNs was also influenced by the insulin loading level. Freezing water was the majority of the absorbed water in the swollen SPH-IPNs and would facilitate drug release. A higher content of *O*-CMC networks could improve water retention of the polymer in response to both compression and time of exposure at 37°C because of the full IPN structure. The *in vitro* and *in vivo* tests showed that the SPH-IPN had no cytotoxicity or mucosal toxicity, and it was deemed biocompatible. These desired features would hopefully meet the requirements of stimuli-responsive drug delivery systems for protein drugs.

References

1. Park, S. E.; Nho, Y. C.; Lim, Y. M.; Kim, H. I. J Appl Polym Sci 2004, 91, 636.
2. Abd El-Rehim, H. A.; Hegazy, E. A.; Abd El-Mohdy, H. L. J Appl Polym Sci 2006, 101, 3955.
3. Zhang, X.; Wang, Y. X.; Wang, S. C. Chem Eng Sci 1996, 51, 3235.
4. Schneider, G. B.; English, A.; Abraham, M.; Zaharias, R.; Stanford, C.; Keller, J. Biomaterials 2004, 25, 3023.
5. Drury, J. L.; Mooney, D. J. Biomaterials 2003, 24, 4337.
6. Dorkoosh, F. A.; Borchard, G.; Rafiee-Tehrani, M.; Verhoef, J. C.; Junginger, H. E. Eur J Pharm Biopharm 2002, 53, 161.
7. Dorkoosh, F. A.; Setyaningsih, D.; Borchard, G.; Rafiee-Tehrani, M.; Verhoef, J. C.; Junginger, H. E. Int J Pharm 2002, 241, 35.
8. Yin, L.; Fei, L.; Cui, F.; Tang, C.; Yin, C. Biomaterials 2007, 28, 1258.
9. Wu, J.; Liu, S.; Heng, P. W.; Yang, Y. J Controlled Release 2005, 102, 361.
10. Careri, G.; Gratton, E.; Yang, P. H.; Rupley, J. A. Nature 1980, 284, 572.
11. Hoffman, A. S.; Afrassiabi, A.; Dong, L. C. J Controlled Release 1986, 4, 213.
12. Quinn, F. X.; Kampff, E.; Smyth, G.; MaBrierty, V. J. Macromolecules 1988, 21, 3191.
13. Liu, W. G.; Yao, K. D. Polymer 2001, 42, 3943.
14. Stuart, B. H. Polym Bull 1994, 33, 681.
15. Capitani, D.; Mensitieri, G.; Porro, F.; Proietti, N.; Segre, A. L. Polymer 2003, 44, 6589.
16. Liu, Y.; Huglin, M. B. Polym Int 1995, 37, 63.
17. Chandy, M. C.; Rajasekharan-Pillai, V. N. Polym Int 1995, 37, 39.
18. Dergunov, S. A.; Nam, I. K.; Doldina, M. K.; Nurkeeva, Z. S.; Shaikhutdinov, E. M. Colloids Surf A 2004, 238, 13.
19. Zhao, Y.; Su, H.; Fang, L.; Tan, T. Polymer 2005, 46, 5368.
20. Flory, P. J. Principles of Polymer Chemistry; Cornell University Press: Ithaca, NY, 1953.
21. Mahdavinia, G. R.; Pourjavadi, A.; Hosseinzadeh, H.; Zohuriaan, M. J. Eur Polym J 2004, 40, 1399.
22. Yoo, M. K.; Sung, Y. K.; Lee, Y. M.; Cho, C. S. Polymer 2000, 41, 5713.
23. Ju, H. K.; Kim, S. Y.; Lee, Y. M. Polymer 2001, 42, 6851.
24. Dorkoosh, F. A.; Verhoef, J. C.; Ambagts, M. H. C.; Rafiee-Tehrani, M.; Borchard, G.; Junginger, H. E. Eur J Pharm Sci 2002, 15, 433.
25. Tranoudis, I.; Efron, N. Contact Lens Anterior Eye 2004, 27, 193.
26. Yang, D.; Liu, Y.; He, L. Petrochem Technol 2003, 32, 133.